

Data acquisition and detector characterization of GEO600

This article has been downloaded from IOPscience. Please scroll down to see the full text article.

2002 Class. Quantum Grav. 19 1399

(<http://iopscience.iop.org/0264-9381/19/7/323>)

View [the table of contents for this issue](#), or go to the [journal homepage](#) for more

Download details:

IP Address: 194.94.224.254

The article was downloaded on 29/11/2010 at 13:02

Please note that [terms and conditions apply](#).

Data acquisition and detector characterization of GEO600

K Kötter^{1,2}, C Aulbert⁵, S Babak⁴, R Balasubramanian⁴, S Berukoff⁵, S Bose⁵, D Churches⁴, C N Colacino^{1,2}, C Cutler⁵, K Danzmann^{1,2}, R Davies⁴, R Dupuis³, A Freise^{1,2}, H Grote^{1,2}, G Heinzl^{1,2}, M Hewitson³, J Hough³, H Lück^{1,2}, M Malec^{1,2}, S D Mohanty⁵, S Mukherjee⁵, S Nagano^{1,2}, M A Papa⁵, D Robertson³, B S Sathyaprakash⁴, B F Schutz⁵, A M Sintes⁵, K A Strain³, I J Taylor⁴, A Vecchio⁶, H Ward³, U Weiland^{1,2}, B Willke^{1,2} and G Woan³

¹ Max-Planck-Institut für Gravitationsphysik, Albert-Einstein-Institut Hannover, Callinstr. 38, 30167, Hannover, Germany

² Institut für Atom- und Molekülphysik, Abteilung Spektroskopie, Callinstr. 38, 30167 Hannover, Germany

³ Department of Physics and Astronomy, University of Glasgow, Glasgow G12 8QQ, UK

⁴ Department of Physics and Astronomy, Cardiff University, Cardiff CF24 3YB, UK

⁵ Max-Planck-Institut für Gravitationsphysik, Albert-Einstein-Institut, Am Mühlenberg 1, 14476 Golm, Germany

⁶ School of Physics and Astronomy, The University of Birmingham, Edgbaston, Birmingham, B15 2TT, UK

E-mail: kbk@mpq.mpg.de

Received 3 October 2001, in final form 2 November 2001

Published 11 March 2002

Online at stacks.iop.org/CQG/19/1399

Abstract

The data acquisition system of the gravitational wave detector GEO600 is recording the first data now. Data from detector subsystems and environmental channels are being acquired. The data acquisition system is described and first results from the detector characterization work are being presented. We analysed environmental influences on the detector to determine noise propagation through the detector. Long-term monitoring allowed us to see long-timescale drifts in subsystems.

PACS numbers: 0480N, 9555Y, 9365

(Some figures in this article are in colour only in the electronic version)

1. Introduction

Detector characterization (DC) of the gravitational wave detector GEO600 [1] is a collaborative work of experimentalists and theorists joined in the *GEO600 DC group*.⁷

⁷ http://www.aei-potsdam.mpg.de/sintes/GEO_DC/

The characterization of GEO600 consists of two phases. In the first phase the goal is to improve the detector performance and bring it to the design sensitivity. It is necessary to identify noise sources and to track down transients in the detector's signals. The primary way of achieving this is the analysis of data from the detector. We are interested in the entire bandwidth of the detector output and not just in the band that is searched for gravitational wave signals. In the second phase we will have to determine thresholds for environmental disturbances to provide vetoes for data analysis. The periods of time where external disturbances dominate the detector output will have to be marked in the recorded data so that they will be ignored in search algorithms for gravitational waves. For this task we have to gain a detailed knowledge of noise propagation in the detector. Detector data and environmental data will be analysed with the aim of generating qualitative and quantitative information about various aspects of system performance, e.g., to investigate sources of lock losses, quantify correlations between different channels, quantify the stability of the data, characterize line noise or look for impulses, bursts and chirp type events that contribute to non-Gaussianity. Based on the experience gained in the understanding of the detector, the so-called *detector characterization robot* (DCR) [2] will be developed to produce well characterized data. For its design several sophisticated tools are being developed [3]. DCR will be a reliable and efficient automated system that will keep track of a variety of parameters in all relevant data channels and detect changes, e.g., transients in the data, changes in power spectral density of a channel or changes in the transfer function between channels. DCR will generate a variety of summary information in order to support future data mining tasks (e.g., to get vetoes). A MySQL database will store the large amount of information produced by the DCR.

The DC group is responsible for generating data that are as free of unwanted instrumental artefacts as possible without compromising detectability of astrophysical signals. Further data conditioning may be required depending on the type of astrophysical signal one is looking for. After filtering through astrophysical signal detection algorithms we will be involved intimately with establishing a confidence level for candidate signals.

The next section will describe the data acquisition system that will gather the data required for this work.

2. GEO600 data acquisition system

The experimental components of GEO600 are installed in three different buildings: the central station and the two endstations to the north and east of the central building. While detector data are only acquired in the central station, environmental monitoring data are recorded in all three buildings. All data channels from the computer supervised detector control system, such as the position and alignment control signals of mirrors, the light power on photodiodes, etc will also be recorded. You can see an overview of all available data acquisition channels in figure 1.

To identify how external disturbances couple into the detector output, a number of environmental sensors were installed in these buildings.

Magnetic and electric fields can couple in the electronic hardware and in the actuators used for controlling the mirror positions of the interferometer. Therefore we installed sensors to monitor these fields. We also have seismic sensors in place to record the motion of the ground. Wind speed and wind direction sensors gather data about weather conditions that could lead to an enhanced level of vibrations acting on the interferometer. Microphones are installed in the cleanrooms close to the vacuum tanks and on the tanks themselves. Acoustic signals could couple to the tanks and mirrors, so they are also a potential source of disturbance

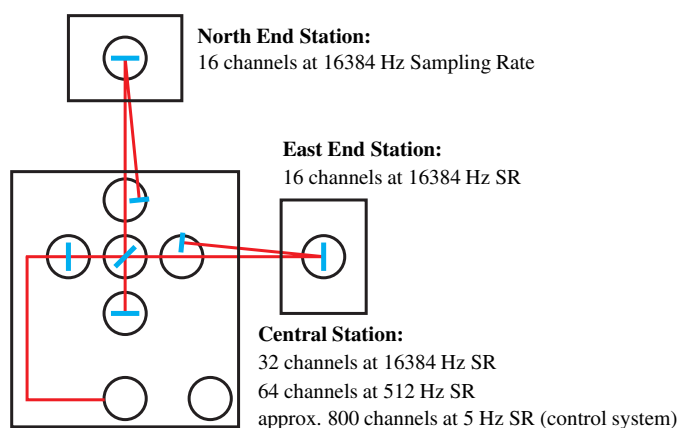


Figure 1. Channels of the GEO600 data acquisition system (DAQS).

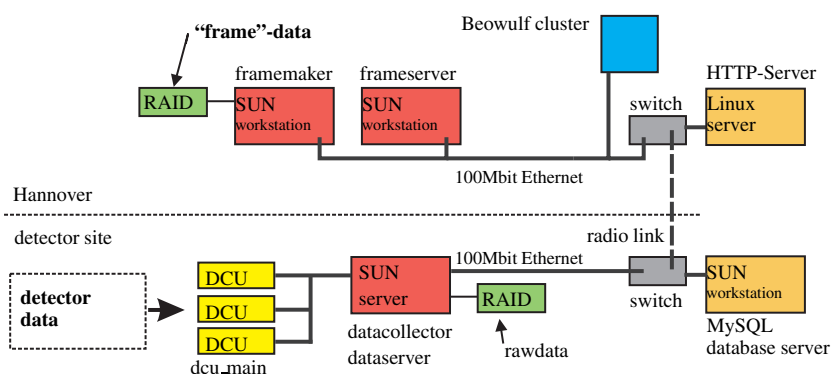


Figure 2. Schematic of the GEO600 DAQS.

to the detector. Changes in temperature, surrounding air pressure and vacuum pressure inside the tanks can lead to slow drifts that will show up in the interferometer output signal, so we are monitoring these environmental influences as well. Though all the control, monitoring and data acquisition electronics is protected from power line noise by uninterruptible power supplies (UPS) that regenerate the 50 Hz/230 V voltage from the incoming line, we are monitoring the supply voltage for any spikes or glitches.

At the current stage detector data are acquired from the mode cleaner only. We can monitor the error point signals showing length fluctuations of the two mode cleaner cavities and the control signal generated from the error point signal of the first cavity that is used to lock the laser frequency to the cavity length [8].

To acquire, store and analyse all these data, a sophisticated data acquisition system is required that is capable of handling a data rate of up to 1 Mbyte s^{-1} and also allows easy access to both stored and real-time data.

An overview of the components of the DAQ system is given in figure 2. The data are acquired by analogue-to-digital converter (ADC) boards installed in a VME-crate. These crates are called DCUs (data collecting units). Further processing is done by a software tool called ‘datacollector’. The configuration of the system (channel names, sampling rates, etc) is stored in a database that can be accessed with a web browser via an HTTP-Interface. After the

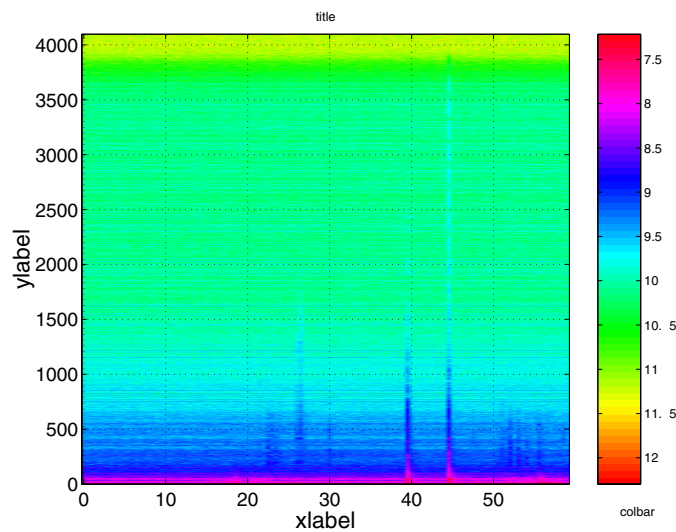


Figure 3. Seismic noise transient in a seismometer signal.

datacollector wrote the data in a preliminary format on a disk array (RAID) these data are then accessed by the ‘framemaker’ software that converts them into the final storage format called ‘frames’. This is a standard data format [4] also used by the gravitational wave detectors LIGO and VIRGO. An automated first analysis step is performed on the data by software running on a Beowulf cluster. Data access is provided by the ‘dataserver’ and ‘frameserver’ software that can deliver data chunks over the network on request.

3. Results

In this section first results from detector characterization work are presented.

3.1. Seismic noise spectrum

To decouple the seismic motion of the ground from the interferometer optics, a sophisticated suspension system [7] is employed in GEO600. As a result the detector sensitivity is limited by seismic noise acting on the mirrors only for frequencies below 40 Hz. But still seismic transients can couple to the mirrors and disturb the measurement.

In figure 3 we can see a spectrogram of a seismometer signal recorded over one minute. At $t = 40$ s and $t = 45$ s transients are visible. They show up as a vertical line in the spectrogram. The transients were generated on purpose by jumping in the central building. Figure 4 illustrates that the seismic motion generated in this event coupled into the mirror motion of the GEO600 mode cleaner cavity. The signal displayed is the feedback going from the mode cleaner cavity length control system to the master laser frequency actuator. It is generated by a Pound–Drever–Hall [5, 6] set-up and is a measure of the relative mirror positions of the mode cleaner cavity.

The transients are clearly visible in this signal. Horizontal lines in the spectrogram starting at the time of the disturbance mark resonances that were excited by this event. The strong horizontal line at 30 Hz is one of the the vertical bounce modes of the mirror suspension.

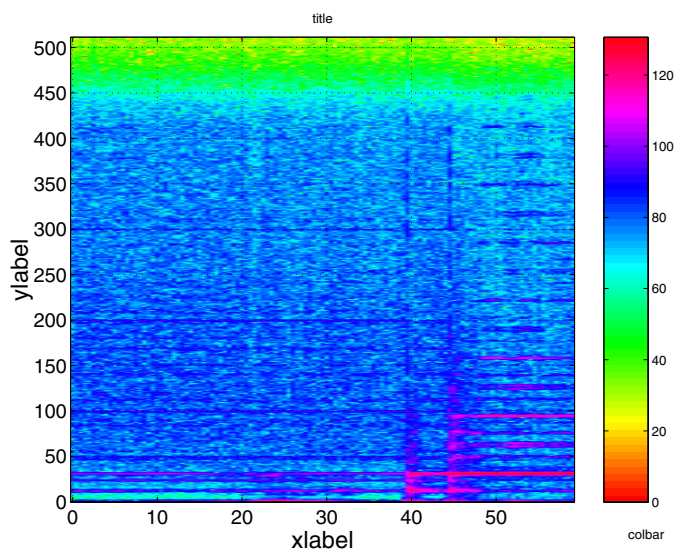


Figure 4. Seismic noise transient in the laser feedback signal (same timescale as in figure 3).

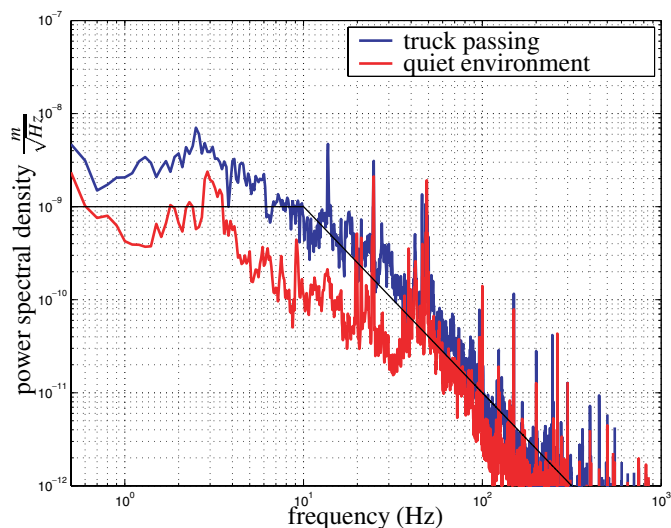


Figure 5. Seismic noise spectra from GEO600 detector site.

To estimate the disturbances on the mode cleaner mirrors caused by seismic motion acting on the detector set-up, measurements of the seismic noise level of the ground have been performed. Commercial motion sensors manufactured by the company *MARK Products* were used.

In figure 5 the linear spectral density of the displacement in vertical direction is displayed. The thin line is the general shape of seismic motion that is similar at many places all over the world: below 10 Hz the linear spectral density has values of about $10^{-9} \text{ m Hz}^{-1/2}$ and above 10 Hz it rolls off proportional to f^{-2} . You can see from the two measurements that the low-frequency contribution of the seismic noise is strongly enhanced by vehicles moving close to the detector site.

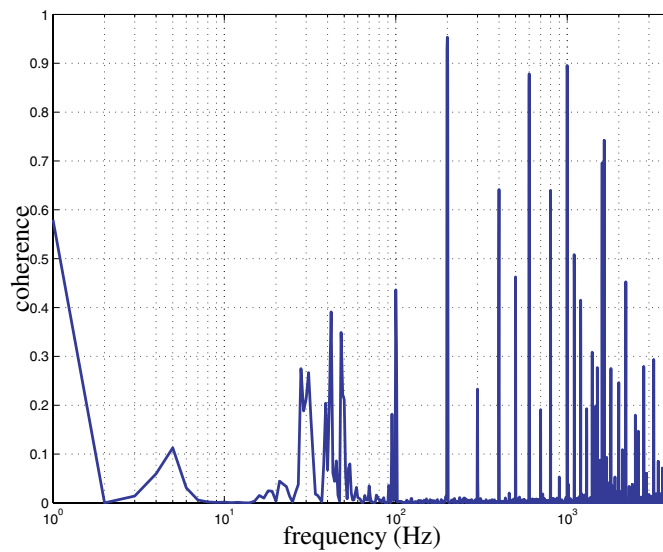


Figure 6. Coherence function between seismic noise and laser feedback signal.

To find out whether there are frequency ranges where the mirror motion is dominated by seismic excitation, we computed a coherence function of the seismic noise and the laser feedback signal from a 10 min stretch of data (see figure 6). The coherence function $C_{xy}(f)$ of two time series $x(t)$ and $y(t)$ is a measure of correlation between the two functions and it can have values between 0 (no correlation between $x(t)$ and $y(t)$) and 1 ($x(t)$ completely determined by $y(t)$).

At frequencies that are multiples of 50 Hz both signals from the seismometer and the laser feedback have large electronic noise contributions due to pick up from the power lines. Therefore, the coherence function has very high values for those frequencies.

Apart from these values the coherence is only significantly higher than zero for frequencies lower than 40 Hz. So we can assume that the suspension of the mode cleaner mirrors provides sufficient decoupling from the ground motion for frequencies higher than 40 Hz at least for linear coupling of the noise. Investigations into non-linear coupling that would upconvert the noise still need to be done.

3.2. Electromagnetic interference

To control the position and alignment of the interferometer mirrors in the GEO600 set-up, we use actuators consisting of a magnet–coil pair. Three of these actuators are acting on each mass from which the mirrors are suspended. As a consequence fluctuations of the environmental magnetic field can couple into the position of the mirrors. These environmental magnetic fields can be of both natural (earth’s magnetic field) and man-made origin (current flow in cables, etc). Magnetic field sensors are installed to record changes in the magnetic field and to deliver data to check correlations between interferometer output and magnetic field changes.

In figure 7 you can see a spectrogram of magnetometer data recorded during a thunderstorm. At $t = 12$ s a lightning strike was observed. This event is clearly visible in the magnetometer data.

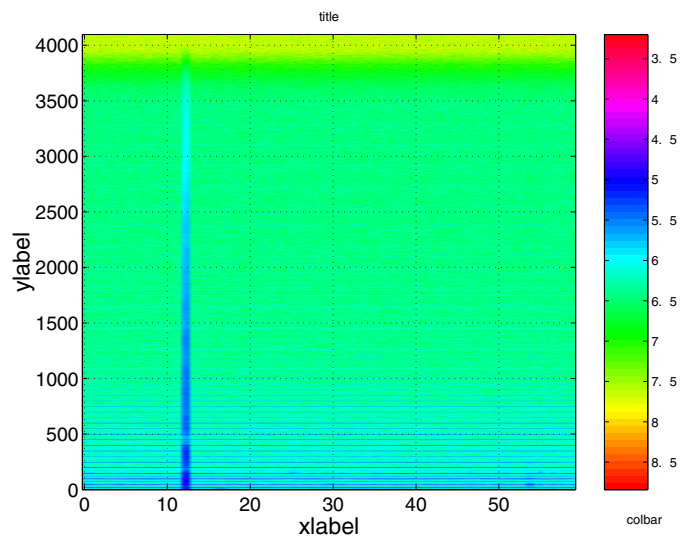


Figure 7. Lightning seen in magnetometer channel.

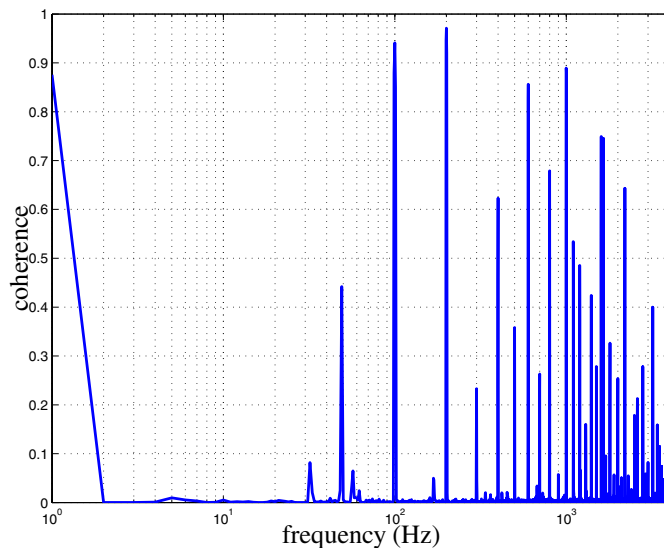


Figure 8. Coherence function of the gradient of the magnetic field and laser feedback signal.

To check whether the magnetic field fluctuations dominate the movement of the mode cleaner mirrors, the coherence of the magnetic field gradient and the laser feedback signal has been computed (see figure 8). The coherence function has high values for frequencies that are multiples of 50 Hz. As already explained earlier this is a consequence of electronic pickup from the electromagnetic field emitted by the power lines. The high coherence value at 0 Hz is due to a DC offset on the sensor output. At 31 Hz there is a small peak in the function. The reason for this could not yet be determined. For all other frequencies the coherence value is low and therefore disturbances caused by magnetic field fluctuations are not dominating the mirror motion.

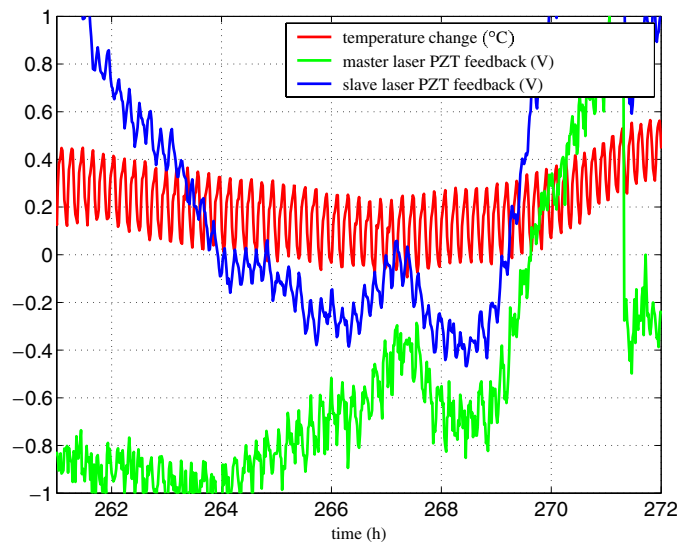


Figure 9. Temperature induced drifts in laser feedback signals.

3.3. Temperature induced drifts

The measurement displayed in figure 9 was made to analyse the long-term behaviour of the laser feedback signals. The master laser feedback keeps the laser locked on the mode cleaner cavity resonance while the slave laser feedback is used to injection lock the high power slave laser on the master laser frequency.

Both signals show a structure that has a period length of about 11 min. This periodic signal is also present in data from the temperature sensor close to the optical bench where the laser system is installed. It turned out that the air conditioning unit in the cleanroom close to the laser set-up is switched on and back off by its controller with a period length of 11 min. Therefore, this structure in the feedback signal of the lasers can be linked to thermal expansion of the resonators that has to be compensated by the control loops.

Apart from this effect we can see a drift on a longer timescale which is not common in the two feedback signals between $t = 261$ h and $t = 266$ h. This can be caused by slow changes in the air pressure, which will only act on the slave laser due to its air-filled cavity whose optical length depends on the refractive index of the air inside. The master laser is not affected since it is an all solid-state laser with a Nd:YAG crystal as a resonator. The common drift between $t = 267$ h and $t = 271$ h indicates a change in the mode cleaner frequency induced by an external disturbance changing its length. The control loops force both lasers to follow this disturbance.

These investigations are only a first step in understanding the subsystems of the detector. In the near future we are planning to extend our analysis of the interferometer output signal.

Acknowledgments

The authors thank *PPARC*, *BMBF* and *Land Niedersachsen* (the state of Lower Saxony) for their financial support.

References

- [1] Danzmann K *et al* 1994 *GEO 600—Proposal for a 600m laser-interferometric gravitational wave antenna* (MPQ Garching)
- [2] Mohanty S D and Mukherjee S 2002 Towards a data and detector characterization robot for gravitational wave detectors *Proc. of the 4th Edoardo Amaldi Conf. on Gravitational Waves (Perth, Western Australia, 8–13 July 2001)* *Class. Quantum Grav.* **19** 1471
- [3] Mohanty S D 2002 Median based line tracker (MBLT): model independent and transient resistant removal of line noise from interferometric data *Proc. of the 4th Edoardo Amaldi Conf. on Gravitational Waves (Perth, Western Australia, 8–13 July 2001)* *Class. Quantum Grav.* **19** 1513
- [4] LIGO Data Group and VIRGO Data Acquisition Group 2000 *Specification of a common data frame format for interferometric gravitational wave detectors* LIGO-T970130-C-E, VIRGO-SPE-LAP-5400-102
- [5] Pound R V 1946 Electronic frequency stabilization of microwave oscillators *Rev. Sci. Instrum.* **17** 490
- [6] Drever R W P, Hall J L, Kowalski F V, Hough J, Ford G M and Munley A J 1983 Laser phase and frequency stabilisation using an optical resonator *Appl. Phys.* **B** **31** 97
- [7] Plissi M V, Torrie C I, Husman M E, Robertson N A, Strain K A, Ward H, Lück H and Hough J 2000 GEO 600 triple pendulum suspension system: seismic isolation and control *Rev. Sci. Instrum.* **71** 2539
- [8] Willke B, Brozek O S, Danzmann K, Fallnich C, Gößler S, Lück H, Mossavi K, Quetschke V, Welling H and Zawischa I 1999 *3rd Edoardo Amaldi Conf.* (New York: American Institute of Physics) p 125